

# Metasomatic Phase Relations in the System CaO-MgO-SiO<sub>2</sub>-H<sub>2</sub>O-NaCl at High Temperatures and Pressures

ROBERT C. NEWTON AND CRAIG E. MANNING

*Department of Earth and Space Sciences, University of California at Los Angeles, Los Angeles, California 90095-1567*

## Abstract

An equation of state of solute silica in NaCl brines at 500 to 900°C and 4 to 15 kbar is formulated by making use of two experimentally determined properties of quartz solubility: the silica molality decreases in direct proportion to the logarithm of the NaCl mole fraction ( $X(\text{NaCl})$ ) at pressures approaching 10 kbar, and the relative silica molality (molality at a given NaCl mole fraction,  $m_x$ , divided by the molality in pure H<sub>2</sub>O at the same P and T,  $m_0$ ) is independent of temperature in the evaluated range. These two properties are expressed in the relation:

$$\log(m_x/m_0)^* = A + BX(\text{NaCl}),$$

where  $\log(m_x/m_0)^*$  denotes the logarithm of the ideal molality ratio, and A and B are functions of pressure, but not temperature or salinity, such that  $B = -1.730 - 1.431 \times 10^{-3}P + 5.923 \times 10^{-4}P^2 - 9.243 \times 10^{-5}P^3$ , and  $A = 0$  at  $P > 10$  kbar, whereas  $A = 0.6131 - 0.1256P + 6.431 \times 10^{-3}P^2$  at  $P \leq 10$  kbar, as derived from fits to experimental data (Newton and Manning, 1999). The parameter A decreases from 0.214 to 0 from 4 to 9.5 kbar, and remains zero to 15 kbar; B decreases from -1.373 to -1.571 from 4 to 15 kbar. With the above relationship defining a variable  $X(\text{NaCl})$ -T-P standard-state of solute silica, the activity of SiO<sub>2</sub> can be replaced by its molality for calculations of mineral-fluid equilibria over most of the conditions for metasomatism in the deep crust and upper mantle. Significant departures from ideality occur only at the lowest pressures, and low salinities.

Calculations on peridotite mineral stability in the simple system CaO-MgO-SiO<sub>2</sub>-H<sub>2</sub>O-NaCl at high T and P show that antigorite, brucite, and diopside are stable at 500°C and pressures of 5 to 15 kbar in the presence of concentrated NaCl solutions at low SiO<sub>2</sub> activities. At 700°C, anthophyllite is stable over a wide range of salinities at 5 kbar with tremolite but not with diopside. The presence of anthophyllite buffers silica solubility at a high, salinity-independent value close to quartz saturation. At 10 and 15 kbar and 700°C, talc replaces anthophyllite as the stable hydrate, and talc-tremolite assemblages buffer SiO<sub>2</sub> fluid concentrations at high values nearly independent of salinity. At 900°C hydrates are unstable and diopside again becomes stable and coexists with enstatite in peridotites. These stability calculations correspond well to the observed progressive metamorphic sequence in peridotite bodies in the Central Alps.

This method of analysis may be useful in interpretation of metamorphosed ultramafic bodies in general, including the basal portions of obducted ophiolitic mantle lithosphere and the mantle wedge above subduction zones. More detailed calculations, including rocks containing feldspars, must take into account the more soluble major components of rocks, especially alkalis, as these will affect the activity coefficient of SiO<sub>2</sub> in NaCl solutions. The solubility of silica in the presence of minerals containing these components must be determined by additional measurements.

## Introduction

MODELING OF MINERAL STABILITY and metasomatism in the Earth's crust and mantle requires detailed knowledge of the thermodynamic properties of natural fluids and dissolved species. A principal source of information is measurements of solubilities of common rock-forming minerals in aqueous solutions, including those containing major amounts of other components such as CO<sub>2</sub> and solu-

ble salts. The most comprehensive solubility data available are for quartz in pure H<sub>2</sub>O. Since SiO<sub>2</sub> is one of the most soluble major components of common rocks at elevated T and P, these data may be used for stability calculations involving common assemblages, especially those low in alkalis, such as ultramafic systems of the upper mantle (Manning, 1995).

An important class of natural fluids is alkali chloride brine. Fluid-inclusion studies have shown

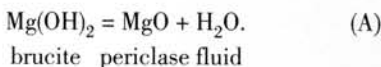
that this type of fluid was involved in the crystallization and subsequent metamorphism of the Duluth Gabbro (Pasteris et al., 1995) and the Zabargad Island (Red Sea) peridotite complex (Sciuto and Ottonello, 1995), as well as many other kinds of igneous and metamorphic rocks. Experimental studies of dilute and concentrated NaCl-KCl solutions (Aranovich and Newton, 1996, 1997) have shown that H<sub>2</sub>O activity decreases rapidly with pressure at temperatures in the range from 500 to 900°C. Above ~2 kbar, a single-phase supercritical solution exists at these temperatures in the system NaCl-H<sub>2</sub>O. The H<sub>2</sub>O activity approaches the square of the mole fraction at pressures above ~5 kbar. The lowered H<sub>2</sub>O activity in concentrated brines has a strong influence in suppressing hydrous minerals in mafic and ultramafic assemblages at high pressures. This property, in addition to changes of SiO<sub>2</sub> solubility with concentration of ionized solutes, could have important consequences for fluid-driven processes at depths greater than ~20 km.

The solubility of quartz in supercritical NaCl solutions has been measured recently over wide ranges in temperature, pressure, and NaCl concentration (Newton and Manning, 1999). These new data show that quartz solubility can be quite simply characterized in concentrated NaCl solutions at high temperatures and pressures, in contrast to its complex behavior in dilute solutions at low pressures (Xie and Walther, 1993). Moreover, quartz solubility is substantial in concentrated NaCl solutions of very low H<sub>2</sub>O activity, in contrast to H<sub>2</sub>O-CO<sub>2</sub> solutions, where it is as much as an order of magnitude lower at comparable H<sub>2</sub>O activities. These properties make possible a simple but comprehensive reconstruction of the thermodynamics of silica solution applicable to the study of brine-mineral interactions in rock systems where silica is the most soluble major rock component.

### Previous Work

#### *The system H<sub>2</sub>O-NaCl*

Aranovich and Newton (1996) determined the H<sub>2</sub>O activity in concentrated NaCl solutions at 2 to 15 kbar and 500 to 900°C by measuring the isobaric temperature depression of the brucite dehydration reaction to periclase:



They found a much greater salinity dependence of the dehydration temperatures at 10 to 15 kbar than at 2 to 4 kbar, indicating much faster decrease of the H<sub>2</sub>O activity with NaCl concentration at high pressures. A fortunate property of the brucite-periclase H<sub>2</sub>O activity monitor is negligibly low solubility of MgO in the H<sub>2</sub>O-NaCl fluids. The dependence of H<sub>2</sub>O activity on NaCl mole fraction, X (NaCl), is well described by the expression:

$$a(\text{H}_2\text{O}) = (1 - X[\text{NaCl}]) / (1 + \alpha X[\text{NaCl}]), \quad (1)$$

where  $\alpha$  is the dissociation parameter, which varies from near 0 at low pressure to nearly 1 at high pressure as aqueous NaCl progressively ionizes. Aranovich and Newton (1996) showed that from 2 to 15 kbar and 600 to 900°C  $\alpha$  is described by

$$\alpha = \exp(4.049 - 2.925/p_0) - 134.2 P/T, \quad (2)$$

with T in K, P in kbar, and  $p_0$ , the density of pure H<sub>2</sub>O at T and P, in gm/cm<sup>3</sup>. Equation 2 illustrates that  $\alpha$  depends on pressure and temperature, but not NaCl concentration. Together, Equations 1 and 2 indicate that H<sub>2</sub>O activity in NaCl solutions decreases rapidly with pressure above ~4 kbar. At 10 kbar and above, H<sub>2</sub>O-NaCl solutions are very nearly ideal mixtures of completely ionized NaCl (Na<sup>+</sup> and Cl<sup>-</sup>) and slightly ionized H<sub>2</sub>O.

#### *The system SiO<sub>2</sub>-H<sub>2</sub>O*

The pioneering studies of quartz solubility by Kennedy (1950) and Morey and Hesselgesser (1951) demonstrated that quartz solubility increases greatly with increasing solution density at temperatures and pressures above the critical point of H<sub>2</sub>O. At temperatures above 1000°C and pressures approaching 10 kbar, the aqueous fluid is so rich in silica that it has almost the constitution of a very hydrous siliceous liquid; indeed, the vapor and liquid phases in the system SiO<sub>2</sub>-H<sub>2</sub>O along the hydrous melting curve of quartz merge and become indistinguishable at a critical end point at 9.6 kbar and 1060°C (Kennedy et al., 1962).

Anderson and Burnham (1965) made the first comprehensive measurements of quartz solubility over extended ranges of P and T: 0.5 to 9.5 kbar and 500 to 900°C. These measurements were made by the weight-loss method in an internally heated gas-pressure vessel. The slow quenching rate of this apparatus limited precision at the highest temperatures at pressures approaching the critical end point, where silica solubility becomes substantial

TABLE 1. Log Molality of  $\text{SiO}_{2,\text{aq}}$  in Equilibrium with Quartz

Pressure, kbar	Temperature, °C								
	500	550	600	650	700	750	800	850	900
4	-0.931	-0.779	-0.641	-0.517	-0.404	-0.303	-0.209	-0.126	-0.049
4.5	-0.904	-0.749	-0.607	-0.479	-0.362	-0.256	-0.159	-0.070	0.011
5	-0.882	-0.723	-0.578	-0.446	-0.326	-0.216	-0.116	-0.024	0.061
5.5	-0.861	-0.700	-0.552	-0.418	-0.295	-0.182	-0.078	0.017	0.103
6	-0.842	-0.679	-0.530	-0.392	-0.267	-0.152	-0.047	0.050	0.140
6.5	-0.826	-0.660	-0.509	-0.370	-0.243	-0.126	-0.018	0.082	0.174
7	-0.810	-0.644	-0.490	-0.350	-0.220	-0.101	0.008	0.110	0.203
7.5	-0.796	-0.629	-0.473	-0.331	-0.200	-0.079	0.032	0.134	0.229
8	-0.783	-0.614	-0.458	-0.314	-0.182	-0.060	0.053	0.157	0.253
8.5	-0.771	-0.600	-0.443	-0.298	-0.166	-0.041	0.072	0.177	0.275
9	-0.759	-0.589	-0.430	-0.284	-0.150	-0.025	0.090	0.197	0.295
9.5	-0.748	-0.576	-0.418	-0.270	-0.134	-0.009	0.107	0.215	0.314
10	-0.738	-0.566	-0.406	-0.257	-0.121	0.006	0.123	0.231	0.332
10.5	-0.729	-0.555	-0.395	-0.246	-0.108	0.019	0.138	0.247	0.348
11	-0.719	-0.546	-0.384	-0.234	-0.096	0.033	0.151	0.261	0.364
11.5	-0.711	-0.536	-0.374	-0.223	-0.084	0.045	0.164	0.275	0.378
12	-0.703	-0.527	-0.364	-0.213	-0.074	0.056	0.176	0.287	0.392
12.5	-0.695	-0.519	-0.356	-0.204	-0.063	0.066	0.188	0.300	0.404
13	-0.687	-0.511	-0.347	-0.194	-0.053	0.077	0.199	0.312	0.417
13.5	-0.680	-0.503	-0.338	-0.185	-0.044	0.088	0.209	0.323	0.428
14	-0.672	-0.495	-0.330	-0.177	-0.035	0.097	0.220	0.333	0.440
14.5	-0.666	-0.488	-0.323	-0.169	-0.027	0.106	0.229	0.343	0.450
15	-0.659	-0.480	-0.315	-0.161	-0.018	0.115	0.238	0.353	0.460

Source: Manning, 1994.

(several weight percent of the fluid). Manning (1994) determined the solubility of quartz over a broad P-T range, 5 to 20 kbar and 500 to 900°C, in a well-calibrated piston-cylinder apparatus with NaCl pressure medium. The rapid quench of this apparatus allows precise measurements by the method of weight loss of small single quartz crystals. Manning (1994) showed that the silica molality of aqueous fluid in equilibrium with quartz at a given temperature increases linearly with the logarithm of the  $\text{H}_2\text{O}$  density. He summarized his data and those of earlier workers in a single solubility equation based on this principle. Table 1 presents his solubility prediction in units of log molality in the ranges 4 to 15 kbar and 500 to 900°C.  $\text{H}_2\text{O}$  densities were

taken from the equation of state of Halbach and Chatterjee (1982).

#### *The system $\text{H}_2\text{O}-\text{SiO}_2-\text{NaCl}$*

Prior to the recent study of Newton and Manning (1999), the only measurements of quartz solubility in NaCl brines at elevated P-T conditions were those of Xie and Walther (1993). The maximum conditions of their study were 2 kbar, 573°C, and NaCl mole fraction of 0.015. Silica concentrations of the fluid were measured by spectroscopic analysis of fluids rapidly extracted from equilibration runs at pressure and temperature (Walther and Orville, 1983). They found that NaCl in solution at 1 kbar and temperatures above 400°C actually enhances the solubility

of quartz relative to pure H<sub>2</sub>O. Such a "salting-in" effect also was found for KCl solutions at 3 kbar and 600°C by Anderson and Burnham (1967). Xie and Walther (1993) demonstrated that there is a threshold temperature, ~300°C at 0.5 kbar and above 400°C at 1 kbar, where salting-in behavior commences.

Newton and Manning (1999) measured quartz solubility in NaCl solutions over broad ranges of P-T-X: 2 to 15 kbar, 500 to 900°C, and salinities up to halite saturation. They used the techniques of Manning (1994), except for fluid analysis by puncture-and-dry weight loss measurements on quenched capsules. At 2 kbar and 700°C, there is a substantial salting-in effect similar to that found by Xie and Walther (1993) at 1 kbar. Quartz solubility at those conditions rises to a maximum at X(NaCl) ~0.1, which is 50% higher than in pure H<sub>2</sub>O. The solubility does not become as low as in pure H<sub>2</sub>O until the NaCl concentration reaches 40 mole%, or 68 wt%. At 10 and 15 kbar, however, there is an exponential decrease of SiO<sub>2</sub> solubility with NaCl mole fraction. At 4.35 kbar, the behavior is intermediate between these extremes. Although an absolute salting-in does not occur at this pressure, a tendency toward solubility enhancement at low X(NaCl) persists.

The combined results of Anderson and Burnham (1967), Xie and Walther (1993), and Newton and Manning (1999) imply that the change from salting-in to salting-out behavior correlates with the pressure-induced decrease of H<sub>2</sub>O activity in NaCl solution, and attendant, progressive ionization of solute NaCl<sup>o</sup> (Newton and Manning, 1999). The simple exponential dependence of quartz solubility on NaCl mole fraction at high pressure is explainable in straightforward terms if the SiO<sub>2</sub> aqueous species, the H<sub>2</sub>O molecules, and the Na<sup>+</sup> and Cl<sup>-</sup> ions together form an ideal mixture—that is, if the ions and molecules mix in the solution without excess enthalpy and excess entropy. By contrast, neutral NaCl<sup>o</sup> dominates at low pressures, evidently leading to the more complex salting-in behavior. The transition from salting in to salting out occurs at densities of pure H<sub>2</sub>O of 0.7 to 0.8 g/cm<sup>3</sup>, or  $\alpha$  ~0.6 to 0.65. The precise mechanism of SiO<sub>2</sub>-solute interaction cannot be elucidated at present.

Another useful property of silica solubility in high-pressure, high-temperature NaCl solutions is that the silica molality at a given NaCl concentration,  $m_x$ , divided by the molality in pure H<sub>2</sub>O at the same P and T,  $m_o$ , is effectively temperature-inde-

pendent at pressures of 4.35 kbar and above. Figure 1 shows the measurements of Newton and Manning (1999) of relative molality at 4.35 and 10 kbar. The corresponding data for 15 kbar lie very close to the 10 kbar data and are not plotted. Least-squares fits to these data at the investigated pressures, combined with interpolation between these pressures, yielded the curves for 4 to 15 kbar in Fig. 1 (Newton and Manning, 1999). The near-ideal behavior of NaCl-H<sub>2</sub>O solutions, described by equation 1, together with the near temperature-independence of the relative SiO<sub>2</sub> molality, makes possible a simple equation of state of solute silica that is useful for practical calculations of mineral stability in the presence of concentrated NaCl solutions.

### Formulation of Activity-Concentration Relations

Figure 2 shows the quartz solubility data of Newton and Manning (1999), plotted as the logarithm of relative silica molality versus NaCl mole fraction. The experimental data at 10 and 15 kbar and all temperatures project through the origin as straight lines and are thus temperature-independent exponential arrays. At very high X(NaCl), realized at 10 kbar in the highest-temperature data, the measurements depart from the linear trend toward lower solubilities. Newton and Manning (1999) proposed that this results from the progressive destabilization of a hydrated solute species, probably H<sub>4</sub>SiO<sub>4</sub>, which would occur at very low H<sub>2</sub>O activities. The 4.35 kbar data depart from linearity at low NaCl concentrations. This behavior reflects the persistence of low-pressure salting-in behavior. At X(NaCl) greater than about 0.2, the logarithm of the solubility ratio decreases linearly as at 10 and 15 kbar, suggesting that solutions of high salinity are simple mixtures even at pressures below 5 kbar.

The data arrays in Figure 2 follow the trend

$$\log (m_x/m_o)^* = A + B X(\text{NaCl}) \quad (3)$$

over their linear ranges. In equation 3,  $\log (m_x/m_o)^*$  is the logarithm of the molality ratio assuming linear behavior predicted by the right-hand side of the equation. This relationship can thus be used to define a standard state for solute silica of unit molality and unit activity in a hypothetical solution that obeys equation 3 and Henry's Law. The activity of SiO<sub>2</sub> thus defined is applicable only at 4–15 kbar, 500–900°C, and X(NaCl) to halite saturation, which

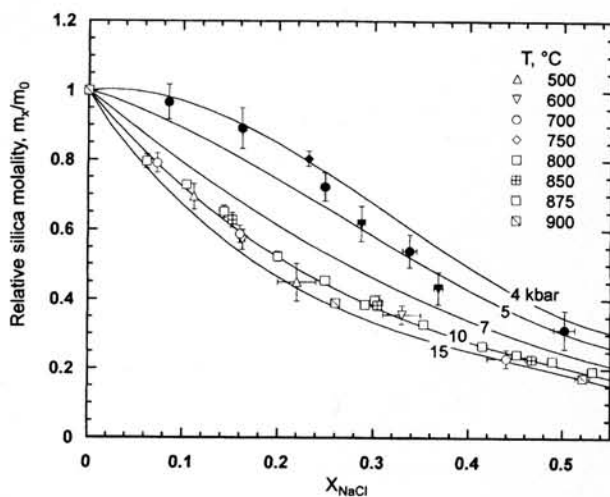


FIG. 1. Relative silica molality in NaCl solutions at pressures of 4 to 15 kbar and 500 to 900°C in equilibrium with quartz. Experimental data of Newton and Manning (1999) at 4.35 kbar (filled symbols) and 10 kbar (open symbols) and the indicated temperatures. The temperature-independent isobars shown are those modeled from the data at all pressures and temperatures by Newton and Manning (1999).

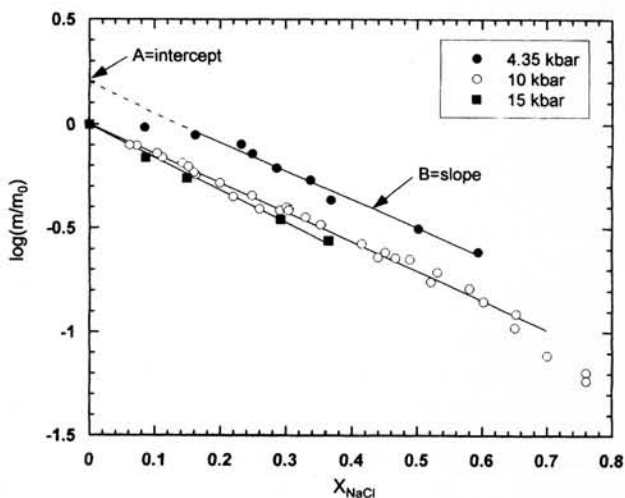


FIG. 2. Data of Figure 1 plotted on a logarithmic scale versus NaCl mole fraction. The data at all temperatures are plotted. The figure illustrates the near temperature-independence of the relative molality. Departure of the 4.35 kbar data from a linear trend occurs at NaCl mole fraction less than 0.2; this is an effect of the tendency toward "salting-in" at low pressures and low salinities (see text). Extrapolation of the linear portion of the 4.35 kbar data to  $X(\text{NaCl}) = 0$  yields the A parameter of equation 2. The B parameter is the slope of the isobar.

reflects the range of the experimental data upon which it is based. At most of these conditions, silica activity will be equal to its molality. Significant departures from ideality relative to this standard state correspond to departures from linear behavior. Such departures are encountered only at the lowest

pressures and NaCl concentrations, and at very high NaCl concentrations at high temperatures.

As illustrated in Figure 2, the A and B parameters correspond to the intercepts and slopes of each isobaric array of solubility data. Expressions for the variations in the slopes and intercepts were derived

TABLE 2. Values of A and B Parameters Used to Calculate Activity Coefficients at Discrete Pressures

Pressure, kbar	A	B
4.0	0.214	-1.373
4.5	0.178	-1.373
5.0	0.146	-1.374
5.5	0.117	-1.376
6.0	0.091	-1.378
6.5	0.068	-1.380
7.0	0.049	-1.383
7.5	0.033	-1.387
8.0	0.020	-1.391
8.5	0.010	-1.397
9.0	0.004	-1.403
9.5	0.000	-1.410
10.0	0.000	-1.418
10.5	0.000	-1.427
11.0	0.000	-1.437
11.5	0.000	-1.449
12.0	0.000	-1.462
12.5	0.000	-1.476
13.0	0.000	-1.492
13.5	0.000	-1.509
14.0	0.000	-1.528
14.5	0.000	-1.548
15.0	0.000	-1.571

by linear least-squares fits to the experimental data at 4.35, 10, and 15 kbar (Fig. 2), combined with interpolation between these pressures. The resulting equations for A and B are:

$$A = 0.6131 - 0.1256P + 6.431 \times 10^{-3}P^2 \quad P \leq 10 \text{ kbar}$$

$$A = 0 \quad P > 10 \text{ kbar};$$

and

$$B = -1.730 - 1.431 \times 10^{-3}P + 5.923 \times 10^{-4}P^2 - 9.243 \times 10^{-5}P^3 \quad P = 4-15 \text{ kbar}$$

The two fit regions for A arise from the observation that nonzero intercepts occur only at  $P < 10$  kbar (Fig. 2). Table 2 gives A and B values at discrete pressures over the P and T ranges of interest. Figure

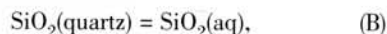
3 illustrates that A has small positive values that decrease to zero with increasing pressure, whereas B becomes progressively more negative as P increases, consistent with the changes in slope and intercept illustrated in Figure 2.

Deviations from ideality for aqueous silica in equilibrium with quartz exist where equation 3 does not describe accurately the experimentally determined values of  $\log(m_x/m_o)$ . Thus, the activity coefficient of solute silica is given by:

$$\log \gamma (\text{SiO}_2) = A + B X(\text{NaCl}) - \log(m_x/m_o). \quad (4)$$

In equation 4,  $\log(m_x/m_o)$  is the value consistent with experimental data (Manning, 1994; Newton and Manning, 1999) as opposed to the ideal value,  $\log(m_x/m_o)^*$ . Comparison of equations 3 and 4 illustrates that the logarithm of the activity coefficient for aqueous silica is simply the difference between  $\log(m_x/m_o)^*$  and  $\log(m_x/m_o)$ . Table 3 gives values of  $\log \gamma (\text{SiO}_2)$  at the range of P and X(NaCl) where nonideality occurs. (We omit consideration of departures from ideality at very high salinity ( $X(\text{NaCl}) > 0.5$ ), because such solutions are likely to be geologically rare.)

The quartz-solution equilibrium is expressed formally by:



for which the standard Gibbs free energy change is a function of temperature, pressure, and salinity, given by the relation:

$$\Delta G_r^\circ / 2.303RT = \log a_{\text{SiO}_2(\text{aq})} = A + BX(\text{NaCl}) + \log m_o \quad (5)$$

The standard state for quartz is unit activity of the pure phase at any pressure and temperature.  $\Delta G_r^\circ$  is interpreted as the Gibbs free energy change when one mole of quartz is dissolved at fixed T and P into a very large quantity of solvent of concentration X(NaCl). For 5 kbar and 700°C, equation 5 and Tables 1 to 3 indicate that the solution reaction in pure H<sub>2</sub>O is attended by a Gibbs free energy change of 3.33 kJ. The corresponding Gibbs free energy change for solution into pure (metastable) molten NaCl is 28.93 kJ. The latter quantity is purely hypothetical in that it implies the existence of a hydrous solute silica species in a completely anhydrous solvent. Nevertheless, the changes in  $\Delta G_r^\circ$  with X(NaCl) illustrate the magnitude of the increased

TABLE 3. Values of  $\log \gamma_{\text{SiO}_2, \text{aq}}$  at Discrete Values of Pressure and  $X_{\text{NaCl}}$ 

Pressure, kbar	XNaCl								
	0.000	0.025	0.050	0.075	0.100	0.125	0.150	0.175	0.200
4.0	0.214	0.179	0.145	0.111	0.076	0.042	0.008	0.000	0.000
4.5	0.178	0.144	0.109	0.075	0.041	0.006	0.000	0.000	0.000
5.0	0.146	0.112	0.077	0.043	0.008	0.000	0.000	0.000	0.000
5.5	0.117	0.082	0.048	0.014	0.000	0.000	0.000	0.000	0.000
6.0	0.091	0.057	0.022	0.000	0.000	0.000	0.000	0.000	0.000
6.5	0.068	0.034	0.000	0.000	0.000	0.000	0.000	0.000	0.000
7.0	0.049	0.014	0.000	0.000	0.000	0.000	0.000	0.000	0.000
7.5	0.033	0.000	0.000	0.000	0.000	0.000	0.000	0.000	0.000
8.0	0.020	0.000	0.000	0.000	0.000	0.000	0.000	0.000	0.000
8.5	0.010	0.000	0.000	0.000	0.000	0.000	0.000	0.000	0.000
9.0	0.004	0.000	0.000	0.000	0.000	0.000	0.000	0.000	0.000
9.5	0.000	0.000	0.000	0.000	0.000	0.000	0.000	0.000	0.000
10.0	0.000	0.000	0.000	0.000	0.000	0.000	0.000	0.000	0.000

free-energy change associated with the dissolution of quartz with increasing salinity.

Calculation of  $\Delta G^\circ$  for quartz at the P and T of interest allows equation 5 to be rewritten in terms of the Gibbs free energy of aqueous silica NaCl-bearing solutions:

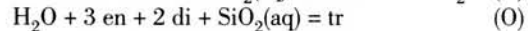
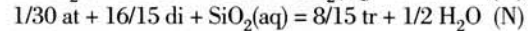
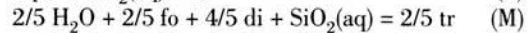
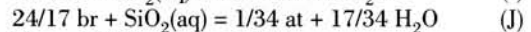
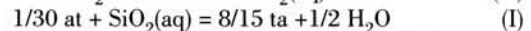
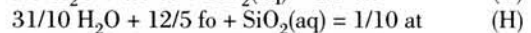
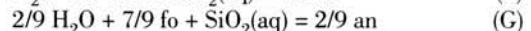
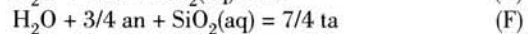
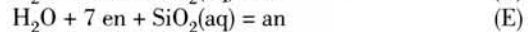
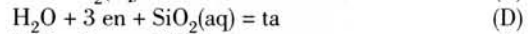
$$\Delta G_{\text{SiO}_2(\text{aq})}^\circ = -2.303RT(A + B X(\text{NaCl}) + \log m_w) + \Delta G_{\text{quartz}}^\circ \quad (6)$$

Equation 6 permits calculation of metasomatic phase relations as a function of  $X(\text{NaCl})$  and silica concentration.

### Application to the System CaO-MgO-SiO<sub>2</sub>-H<sub>2</sub>O-NaCl

The above formulation of the thermodynamics of quartz solubility may be applied to a simple ultramafic system that models the mineralogy of the upper mantle, the basal sections of ophiolites, and ultramafic intrusions in the crust with saline pore fluids, at elevated P-T conditions ( $T > 500^\circ\text{C}$ ;  $P > 5$  kbar). As an example of calculation, diagrams of  $\log m(\text{SiO}_2)$  versus  $X(\text{NaCl})$  are constructed at 500, 700, and  $900^\circ\text{C}$ , and 5, 10, and 15 kbar (Fig. 4). The minerals considered are, in addition to quartz (qz), diopside (di), tremolite (tr), enstatite (en), forsterite (fo), talc (ta), anthophyllite (an), antigorite (at), bru-

cite (br), and periclase (pe). The non-peridotite CMSH minerals wollastonite, monticellite, larnite, portlandite, and lime were not considered. Fifteen isobaric, isothermal univariant equilibria, including reactions A and B, were found to have stable portions in the ranges of 5 to 15 kbar and 500 to  $900^\circ\text{C}$ :



The reactions are normalized to one  $\text{SiO}_2(\text{aq})$  for convenience. The  $\text{SiO}_2$ -independent reaction A is a consequence of K and L. Calculations were performed with the Holland and Powell (1998) thermodynamic data set and the Halbach and Chatterjee (1982) equation of state of  $\text{H}_2\text{O}$ , for which we adopted a standard state of unit activity for the pure phase at all T and P. Activity of  $\text{H}_2\text{O}$  was calculated

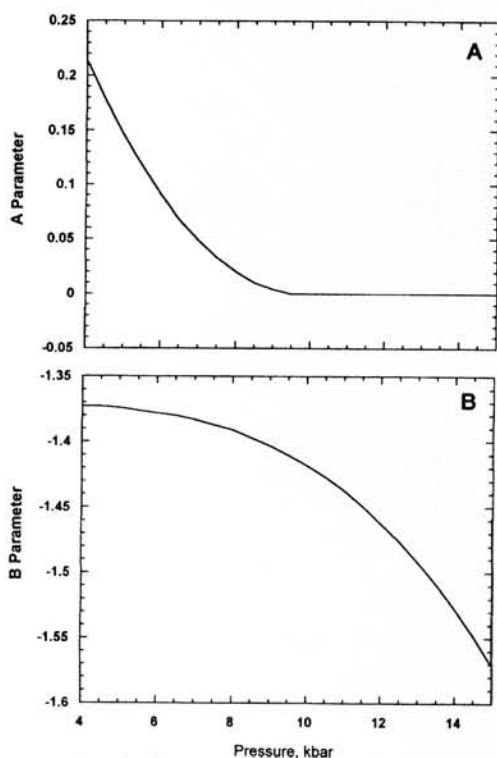


Fig. 3. Variation in the A and B parameters in equation 2 with pressure (see text).

from Aranovich and Newton (1996), with extrapolation to 500°C.

Figures 4A–4J illustrate some features of the calculations. At 5 kbar, the effect of  $\gamma(\text{SiO}_2) > 1$  is seen in the non-linear reaction curves at low salinity. This behavior is a carry-over from the salting-in effect at low pressure and low salinity where NaCl° is predominantly associated. At 500°C, forsterite, antigorite, talc, brucite, tremolite, and diopside are stable phases at 5 to 15 kbar, and enstatite and periclase are not stable in that range. A small range of stability of reaction J was found at low salinity at 15 kbar. Saline solutions are restrictive to antigorite stability. Maximum salinities are limited by halite saturation near a NaCl mole fraction of 0.2. At 700°C, anthophyllite is stable at 5 kbar. Its stability relative to enstatite is almost unaffected by salinity. A small range of stability of reaction G was found at low salinity. Salinity is extremely inimical to talc stability at 5 kbar, but the talc field expands strongly at 10 and 15 kbar, and anthophyllite disappears. Enstatite is stable throughout the pressure range at

700°C. Periclase is stable along with brucite. At 900°C, the only stable hydrate is brucite at 15 kbar. At this temperature diopside can coexist with enstatite or forsterite over the complete range of silica activity and NaCl concentration.

### Geological Applications

The major application of the present analysis is to middle- to high-grade metamorphism of ultramafic bodies, principally alpine peridotites. Lower-grade parageneses pertinent to serpentinization were formed at temperatures below the applicability of the present work. Trommsdorff and Evans (1974) described ultramafic assemblages in a progressive metamorphic suite from the central Alps. Evans and Trommsdorff (1974) inferred pressures of metamorphism of these rocks near 7 kbar. Their lowest temperature assemblage of chrysotile-brucite would be stable at temperatures much below 500°C. Antigorite-brucite-diopside is found in higher-grade metaperidotites, but would indicate temperatures below 500°C if pore solutions are even moderately salty. Figures 4A–4C show that saline fluids are prejudicial to this assemblage, since the field boundaries of brucite and antigorite diverge strongly with increasing salinity. An antigorite-out isograd in the Alps was thought to occur between the staurolite and sillimanite isograds, i.e., between 500 and 700°C, consonant with Figure 4. Successively higher grade assemblages in the Alpine metaperidotites include talc-tremolite-enstatite, tremolite-forsterite-enstatite, and diopside-forsterite-enstatite. Figure 4 illustrates that these assemblages are all stable at 700°C over a range of pressure and NaCl concentration.

Figure 4 indicates that pore-fluid salinity and silica activity have to be taken into account in the assessment of metamorphic grade. Moreover, certain mineral assemblages are diagnostic of a restricted range of silica activity and salinity. For instance, at 500°C and 5 kbar, the assemblage forsterite + tremolite requires high  $X(\text{NaCl})$  and low silica concentrations. Similarly, the anhydrous peridotite assemblage forsterite-enstatite-diopside can occur at 700°C and 10 kbar in the presence of aqueous pore fluids only if they are very salty ( $X(\text{NaCl}) < 0.3$ ). In general, high fluid salinity and low silica activity have the same effects as increasing temperature in favoring anhydrous and low-silica assemblages. Periclase and brucite occur at such low  $\text{SiO}_2$  activities that their presence is not likely in



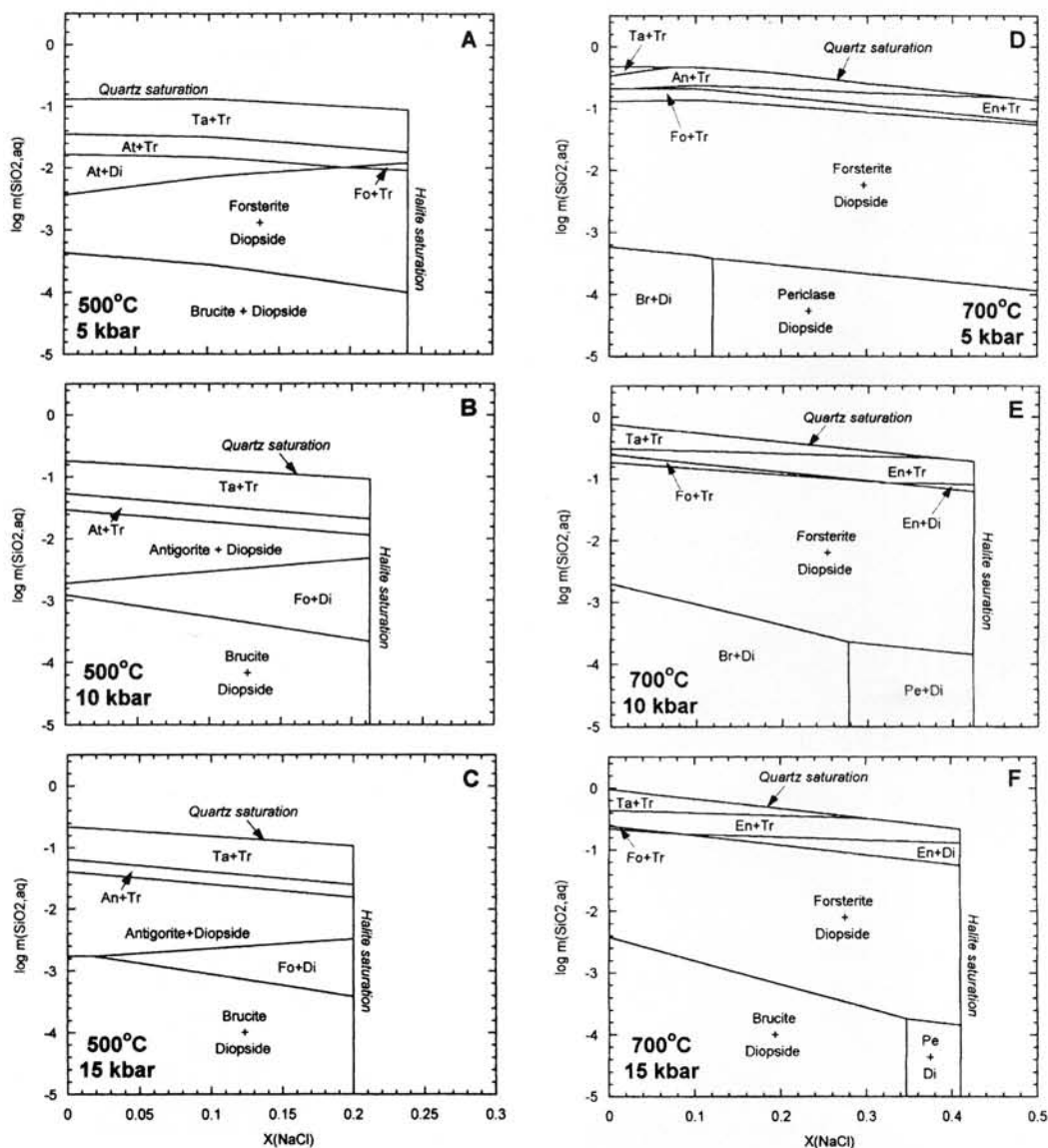


Fig. 4. A–I (G–I on facing page). Stability relations and silica solubilities of model fluid-saturated peridotite assemblages in the simple system  $\text{CaO-MgO-SiO}_2\text{-H}_2\text{O-NaCl}$  at various P-T conditions calculated with the present  $\text{SiO}_2$  equation of state and the thermodynamic data for the minerals of Holland and Powell (1998).  $\text{H}_2\text{O}$  fugacities are from Halbach and Chatterjee (1982).  $\text{H}_2\text{O}$  activities in NaCl solutions are from Aranovich and Newton (1996). Mineral abbreviations: an = antigorite; at = anthophyllite; br = brucite; di = diopside; en = enstatite; fo = forsterite; pe = periclase; ta = talc; tr = tremolite.

high-grade peridotites of an initial forsterite-enstatite-diopside assemblage.

The phase relations depicted in Figure 4 also aid interpretation of paragenetic relations. Evans and Trommsdorff (1974) regarded anthophyllite in the

Val d'Efra metaperidotite as a retrograde phase, possibly formed in decompression below 7 kbar of an original talc-enstatite assemblage. Figures 4D and 4E uphold this concept, and show that anthophyllite would be stable at 5 kbar and 700°C with fluids of a

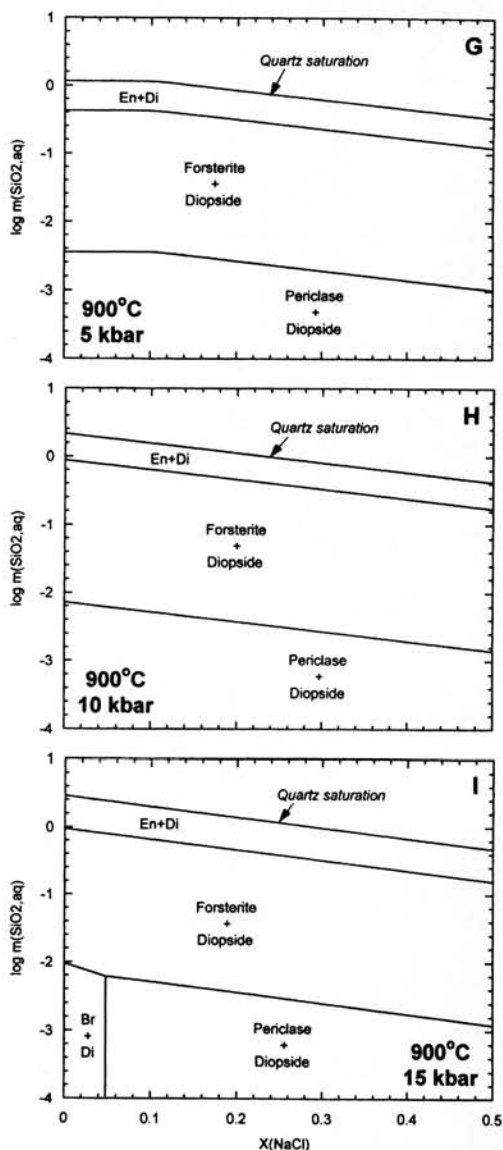


Fig. 4. Continued.

wide range of salinity. Anthophyllite indicates silica molality near 0.2, nearly independent of salinity. The high silica activity, close to quartz saturation, indicates considerable silica metasomatism of an originally ultramafic body. Another possibility suggested by Evans and Trommsdorff (1974) for anthophyllite formation at Val d'Efra is introduction of iron, which could stabilize anthophyllite relative to talc, a phase restrictive to Fe. NaCl solutions could

be effective in this regard, as they readily dissolve and transport Fe oxides under high-grade metamorphic conditions (Chou and Eugster, 1977).

The major utility of the present type of analysis may be in quantifying the amounts,  $H_2O$  activities, and silica-transporting abilities of metamorphic fluids active in the metamorphism of peridotite bodies. The fact that these bodies often are profoundly metasomatic in character indicates that  $SiO_2$  activity in fluids of various types coexisting with peridotite assemblages is one of the most important parameters determining their mineralogy. The present calculations are necessarily restricted to systems where  $SiO_2$  is the most soluble component at elevated temperatures and pressures. The analysis may be extended to systems with other soluble components, including alkalis, when additional solubility data in feldspar-bearing assemblages become available. Hydrogen ion potential is another important parameter that will have to be characterized experimentally before a comprehensive account of the solubilities can be erected (Anderson and Burnham, 1983).

### Acknowledgments

Primary funding of this project was from a National Science Foundation grant for the study of mineral-fluid interactions, #EAR-9405999. We thank D. Bird, T. Fridriksson, and P. Neuhoff for constructive review of the manuscript.

### REFERENCES

- Anderson, G. M., and Burnham, C. W., 1965, The solubility of quartz in supercritical water: *Amer. Jour. Sci.*, v. 263, p. 494-511.
- \_\_\_\_\_, 1967, Reactions of quartz and corundum with aqueous chloride and hydroxide solutions at high temperatures and pressures: *Amer. Jour. Sci.*, v. 265, p. 12-27.
- \_\_\_\_\_, 1983, Feldspar solubility and the transport of aluminum under metamorphic conditions: *Amer. Jour. Sci.*, v. 283-A, p. 283-297.
- Aranovich, L. Ya., and Newton, R. C., 1996,  $H_2O$  activity in concentrated NaCl solutions at high pressures and temperatures measured by the brucite-pericase equilibrium: *Contrib. Mineral. Petrol.*, v. 125, p. 200-212.
- \_\_\_\_\_, 1997,  $H_2O$  activity in concentrated KCl and KCl-NaCl solutions at high temperatures and pressures measured by the brucite-pericase equilibrium: *Contrib. Mineral. Petrol.*, v. 127, p. 261-271.

- Chou, I-M., and Eugster, H. P., 1977, Solubility of magnetite in super-critical chloride solutions: *Amer. Jour. Sci.*, v. 277, p. 1296-1314.
- Evans, B. W., and Trommsdorff, V., 1974, Stability of enstatite + talc, and  $\text{CO}_2$  metasomatism of metaperidotite, Val d'Efra, Lepontine Alps: *Amer. Jour. Sci.*, v. 274, p. 274-296.
- Halbach, H., and Chatterjee, N. D., 1982, An empirical Redlich-Kwong-type equation of state for water to 1000°C and 200 kbar: *Contrib. Mineral. Petrol.*, v. 79, p. 337-345.
- Holland, T. J. B., and Powell, R., 1998, An internally consistent thermodynamic data set for phases of petrologic interest: *Jour. Metamor. Geol.*, v. 16, p. 309-344.
- Kennedy, G. C., 1950, A portion of the system silica-water: *Econ. Geol.*, v. 45, p. 629-653.
- Kennedy, G. C., Wasserburg, J. G., Heard, H. C., and Newton, R. C., 1962, The upper three-phase region in the system  $\text{SiO}_2\text{-H}_2\text{O}$ : *Amer. Jour. Sci.*, v. 260, p. 501-521.
- Manning, C. E., 1994, The solubility of quartz in  $\text{H}_2\text{O}$  in the lower crust and upper mantle: *Geochim. et Cosmochim. Acta*, v. 58, p. 4831-4839.
- , 1995, Phase-equilibrium controls on  $\text{SiO}_2$  metasomatism by aqueous fluids in subduction zones: Reaction at constant pressure and temperature: *INT. GEOL. REV.*, v. 37, p. 1074-1093.
- Morey, G. W., and Hesselgesser, J. M., 1951, The solubility of some minerals in supercritical steam at high pressures: *Econ. Geol.*, v. 46, p. 821-835.
- Newton, R. C., and Manning, C. E., 1999, Quartz solubility in concentrated NaCl solutions at deep crust-upper mantle metamorphic conditions: 2-15 kbar and 500-900°C: *Geochim. et Cosmochim. Acta* (submitted).
- Pasteris, J. D., Harris, T. N., and Sassani, D. C., 1995, Interactions of mixed volatile-brine fluids in rocks of the southwestern footwall of the Duluth Complex, Minnesota—evidence from aqueous fluid inclusions: *Amer. Jour. Sci.*, v. 295, p. 125-172.
- Sciuto, P. F., and Ottonello, G., 1995, Water-rock interaction on Zabargad Island, Red Sea—a case study. I. Application of the concept of local equilibrium: *Geochim. et Cosmochim. Acta*, v. 59, p. 2187-2206.
- Trommsdorff, V., and Evans, B. W., 1974, Alpine metamorphism of peridotitic rocks: *Schweiz. Mineral. Mitteil.*, v. 54, p. 333-354.
- Walther, J. V., and Orville, P. M., 1983, The extraction-quench technique for determination of the thermodynamic properties of solute complexes. Application to quartz solubility in fluid mixtures: *Amer. Mineral.*, v. 68, 731-741.
- Xie, Z., and Walther, J. V., 1993, Quartz solubilities in NaCl solutions with and without wollastonite at elevated temperatures and pressures: *Geochim. et Cosmochim. Acta*, v. 57, p. 1947-1955.